

# Mineralised Collagen Scaffolds Loaded with Stromal Cell-derived Factor-1 Improve Mandibular Bone Regeneration

Yan LIU<sup>1</sup>, Shuai LIU<sup>1</sup>, Yu FU<sup>1</sup>, Da Tong CHANG<sup>1</sup>, Yan Heng ZHOU<sup>1</sup>

**Objective:** *To create an in situ matrix environment conducive to stem cells from host bone marrow to promote bone regeneration.*

**Methods:** *Three-dimensional porous, mineralised collagen (MC) scaffolds were prepared using a freeze-drying process. The microstructure of scaffolds was observed by field emission scanning electron microscopy. The Bose BioDynamic test system was applied to examine their mechanical properties in wet conditions. The effect of scaffolds loaded with stromal cell-derived factor-1 $\alpha$  (SDF-1 $\alpha$ ) on migration of stem cells was assessed using a 24-well transwell system. SDF-1 $\alpha$ -loaded scaffolds were implanted in the critical size defect in rats and histological staining was used to evaluate the new bone formation.*

**Results:** *Mechanical testing showed that the MC scaffold featured an increased Young's modulus compared with the pure collagen (Col) scaffold in wet conditions. In addition, the MC scaffold loaded with SDF-1 $\alpha$  chemokine improved bone marrow stromal cells' migration. When implanted in mandibular bone defects with 5 mm diameter, the MC scaffolds containing SDF-1 $\alpha$  significantly improved the formation of new bone and blood capillaries within the scaffolds, compared with the SDF-1 $\alpha$ -loaded Col scaffolds and the control group.*

**Conclusion:** *The mineralised collagen scaffolds loaded with SDF-1 $\alpha$ , which creates a matrix environment conducive to stem cell migration, can be exploited to improve bone self-repair as an alternative to contemporary cell seeding approaches.*

**Key words:** *mineralised collagen, scaffold, stromal cell-derived factor-1, mandibular bone, regeneration*

**B**one defects resulting from tumor, trauma, or inflammation usually require reconstruction, which remains a major clinical problem<sup>1-3</sup>. Present therapies including autologous, homologous or heterologous bone grafts, and implants of different biomaterials have not been able to reach satisfactory effects<sup>3-7</sup>. Recently,

bone tissue engineering (TE) has become an alternative strategy to regenerate lost bone<sup>8</sup>. The principle of TE is to employ biocompatible materials or scaffolds seeded with stem cells and/or loaded with appropriate growth factors to promote bone repair and regeneration<sup>9,10</sup>.

Porous biodegradable polymers are widely used in TE as a temporary support for cell growth and tissue regeneration<sup>11,12</sup>. The collagen scaffold, which has a similar chemical constitution and biological properties as natural bone tissue, is drawing more and more attention<sup>13-15</sup>. As TE scaffolds require architecture that balances function and strength, mineralised collagen has a promising potential for its inherent biocompatibility and strength<sup>16-18</sup>. In our previous study, we have proven that biomimetic, mineralised collagen can improve cell growth, proliferation and osteogenic differentiation with prominent nanomechanical properties<sup>16</sup>. However, despite these initial *in vitro* studies<sup>16,17,19</sup>,

<sup>1</sup> Center for Craniofacial Stem Cell Research and Regeneration, Department of Orthodontics, Peking University School and Hospital of Stomatology, Beijing, P.R. China.

**Corresponding author:** Dr. Yan Heng ZHOU, Center for Craniofacial Stem Cell Research and Regeneration, Department of Orthodontics, Peking University School and Hospital of Stomatology, #22 Zhongguancun Nandajie, Haidian District, Beijing 100081, P.R. China. Tel: 86-10-82195728; Fax: 86-10-82195336. E-mail: yanhengzhou@gmail.com

This work was supported by the Projects of International Cooperation and Exchanges (No. 2010DFB32980) and the National Science Foundations of China (Nos. 81201198 and 30973360).

much remains to be investigated regarding the effect of the mineralised collagen scaffold on bone regeneration.

Scaffold-based delivery of signaling molecules that stimulate cell migration, growth and differentiation is another essential factor for TE<sup>20</sup>. Stromal cell-derived factor-1 $\alpha$  (SDF-1 $\alpha$ ) is a ligand for the CXCR4 chemokine receptor, which plays a major role in cell trafficking and homing of host stem cells to injured tissues<sup>21</sup>. Furthermore, SDF-1 $\alpha$  molecules are positively charged at pH 7.4, which can be electrostatically bound to the negatively charged carboxyl groups on the surface of the mineralised collagen scaffold<sup>22</sup>. Therefore, in the present study, we hypothesise that the mineralised collagen scaffold loaded with SDF-1 $\alpha$  may improve bone regeneration by attracting host bone marrow stromal cells to defect area.

## Materials and methods

### *Preparation of collagen scaffolds*

The biomimetic, MC scaffolds were prepared as described previously<sup>16</sup>. Briefly, type I tropocollagen solution from rat tails (BD Biosciences, 8.94 mg/mL) contained in a dialysis membrane (3,500 Da) was immersed in simulated body fluid (SBF, 136.8 mM NaCl, 4.2 mM NaHCO<sub>3</sub>, 3.0 mM KCl, 1.0 mM K<sub>2</sub>HPO<sub>4</sub>·3H<sub>2</sub>O, 1.5 mM MgCl<sub>2</sub>·6H<sub>2</sub>O, 2.5 mM CaCl<sub>2</sub>, 0.5 mM Na<sub>2</sub>SO<sub>4</sub>, and 3.08 mM Na<sub>3</sub>N, pH = 7.0) as a phosphate source 37 °C. Set Type I white Portland cement (PC, Lehigh Cement) was used as a calcium source. In the presence of SBF, PC continuously released calcium and hydroxyl ions. The pH of the salts/collagen solution increased from 5 to 9.5. To prepare pure collagen (Col) scaffolds, the tropocollagen solution was directly dialysed using a phosphate buffer saline (PBS, 0.1 M) at 37 °C. After 3 days, the fibrillised collagen was immersed in deionised water to remove remnant salts.

To prepare porous scaffolds, the fibrillised collagen was collected by centrifugation, mixed with PBS and stirred up until a castable suspension was formed. Then, the suspension was filled into the cavities of 48-well polystyrene culture dishes and frozen at -30°C for 24 h. The samples were lyophilised and cross-linked with 1-ethyl-3-(3-dimethylaminopropyl)-carbodiimide (0.3 M)/ N-hydroxysuccinimide (0.06 M) for 4 h to stabilise the scaffolds. Then, the scaffolds were rinsed thoroughly in deionised water, 1% glycine solution, once again in water and finally lyophilised for use.

### *Field emission scanning electron microscopy (FE-SEM) examination*

The lyophilised samples were mounted on aluminum stubs and sputter-coated with gold for 2 min at 20 mA. The microstructure of samples was observed by FE-SEM (Hitachi S-4800) at 15 kV. The elemental analysis of mineralised collagen was performed by Energy Dispersive Spectroscopy (EDS) coupled to the FE-SEM.

### *Mechanical testing*

Cyclic loading experiments were performed using a Bose ELF 5200 BioDynamic test system (Bose) in wet conditions. The scaffolds (6 mm in thickness and 8 mm in diameter) were soaked in PBS for 24 h before testing. Then the wet scaffolds were compressed 50 times to half of their initial height by maintaining a cross-head speed of 1 mm/min. Young's modulus was calculated from the slope of a linear fit to the elastic range of the stress-strain curve and presented as mean  $\pm$  standard deviation.

### *Cell isolation and cultivation*

Three-week-old male SD rats (90 to 100 g) were obtained from the Department of Laboratory Animal Science, Peking University Health Science Center (Beijing, China). All procedures concerning animal use were approved by the Peking University Institutional Animal Care and Use Committee (No. LA2012-77). Rat bone marrow stromal cells (BMSCs) were isolated and cultured by the method described by Maniopoulos using their plastic adherence capability<sup>23</sup>. Briefly, both ends of the femora were cut off at the epiphysis and the bone marrow was flushed out with 10 ml PBS. Cells were cultured in Alpha Modification of Eagles Medium ( $\alpha$ -MEM, Gibco BRL) containing 20% FBS (Hyclone), 100 U/mL penicillin and 100  $\mu$ g/mL streptomycin, supplemented with 2 mM Glutamine (Glu, Gibco), 55  $\mu$ M 2-ME (Gibco) and 0.1 mM L-ascorbic acid phosphate (Wako) at 37 °C in an atmosphere of 5% CO<sub>2</sub>. The medium was changed after 48 h to remove non-adherent cells and was then renewed three times a week. When 80 to 90% confluence was reached, BMSCs were released from the culture substratum using trypsin/EDTA (0.25% w/v trypsin, 0.02% EDTA), and were moved to dishes (10 cm in diameter) at 1.0 $\times$ 10<sup>6</sup> cells/ml in 10 ml. The third passage BMSCs were used for this study.

### *In vitro cell homing*

The effect of different collagen scaffolds loaded with recombinant murine SDF-1 (R&D Systems) on migration of BMSCs was assessed using a 24-well transwell system (Corning Costar, MA, USA)<sup>20</sup>. The third passage BMSCs with the number of  $2 \times 10^4$  in 100 ml  $\alpha$ -MEM) were placed in the upper chamber. The sterilised collagen scaffolds loaded with 120 ng SDF-1 were put in the lower chamber, which contained 600 ml  $\alpha$ -MEM supplemented with 1% BSA. For the negative control (NC) group, only 600 ml  $\alpha$ -MEM supplemented with 1% BSA was added into the lower chamber. The growth medium of the positive control (PC) consisted of 200 ng/ml of SDF-1 $\alpha$  and 600  $\mu$ l of  $\alpha$ -MEM supplemented with 1% BSA. After 16 h of incubation, the cells were fixed with 10% formaldehyde for 30 min. The upper surface of the transwell was scraped free of cells and debris. Cells that migrated through the pores of the transwell membrane to the bottom of the transwell were stained with crystal violet and counted in five randomly-selected fields for each membrane ( $20 \times$  magnification). The data was expressed as mean  $\pm$  standard deviation (SD) and confirmed in three independent experiments. Statistical analysis between groups was performed by one-way ANOVA at  $\alpha = 0.05$ .

### *Animal experiments*

Twelve male SD rats (150 to 200 g, 6- to 8-weeks-old) were used in this study. The animals were anaesthetised by intraperitoneal injection of pentobarbital (Nembutal 4.5 mg/100 g). Incision along the left mandible was made on the skin, followed by masseter muscle dissection and periosteum incision. A critical size defect (CSD) of 5 mm diameter was then created with a bur cooled continuously by 0.9% saline solution irrigation on the ascending ramus of the mandible. A total of 12 mandibular defects were randomly divided into three groups that received the following implants:

- Control group without any scaffolds
- Collagen scaffolds loaded with 200 ng/ml SDF-1 $\alpha$  (Col group)
- MC scaffolds loaded with 200 ng/ml SDF-1 $\alpha$  (MC group)

The wound was closed in layers using 6-0 sutures. All rats were sacrificed after 12 weeks.

### *Histological evaluation*

All the tissues from the original defect area of each group were fixed with 10% formalin for 24 h, and decalcified

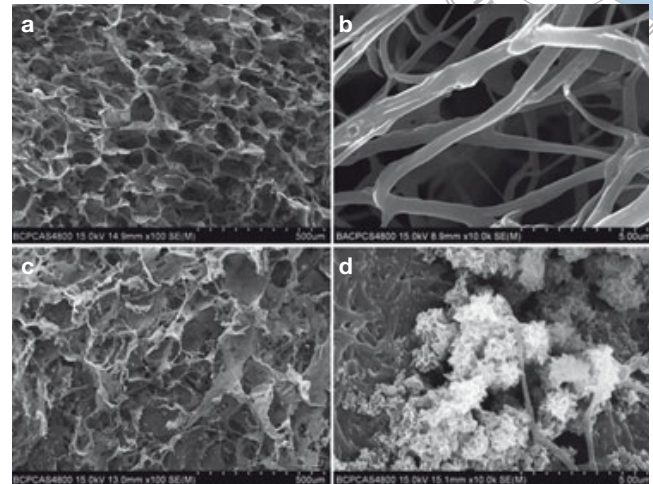


**Fig 1** Microstructure of Col and MC scaffolds observed by FE-SEM. (a) Col scaffold with even porosity ( $118.2 \pm 37.2 \mu\text{m}$ ). (b) High magnification of (a). (c) MC scaffold with uneven porosity ( $108.3 \pm 43.7 \mu\text{m}$ ). (d) High magnification of (c).

in 10% EDTA for 8 weeks. Samples were then embedded in paraffin and serial sections were made. Three randomly selected cross-sections from each implant were stained with hematoxylin and eosin (HE). The new bone formation was assessed by Goldner's Masson trichrome staining. The stained slides were observed using a light microscope (Carl Zeiss).

## **Results**

### *Microstructure of collagen scaffolds*

As shown in Fig 1, three-dimensional (3D) porous scaffolds were produced by a freeze-drying process. The Control scaffold showed uniform pores with diameter of  $118.2 \pm 37.2 \mu\text{m}$ , while uneven pores with diameter of  $108.3 \pm 43.7 \mu\text{m}$  were formed in the MC scaffold. After 3 days, collagen molecules self-assembled into interconnecting nanofibers ( $268.9 \pm 66.0 \mu\text{m}$ ) in PBS. In the crystallization system, flower-like apatites ( $1.7 \pm 0.3 \mu\text{m}$ ) deposited around the collagen nanofibres. This may lead to a decrease of the MC scaffold porosity. The chemical composition analysis of the MC scaffold was carried out by EDS mapping (Fig 2). The main composition was similar to natural bone and Ca and P atoms have similar distributions, with the Ca-to-P ratio of approximately 1.6.

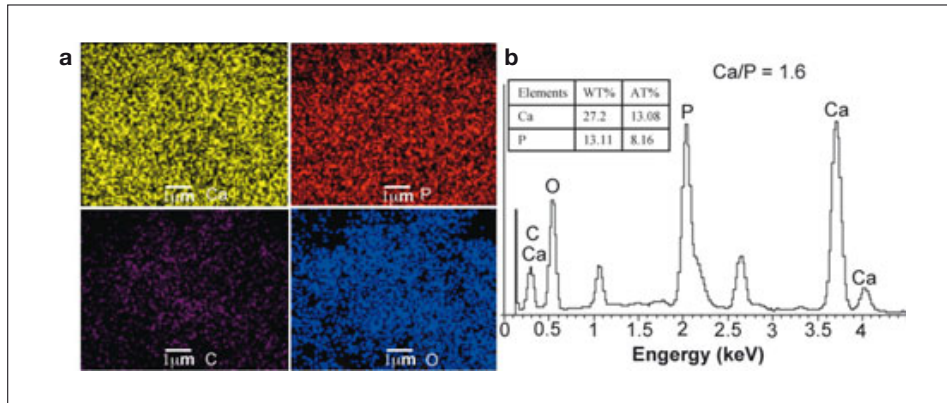


**Fig 2** Chemical composition analysis of MC scaffold by EDS mapping. (a) Element distribution maps. (b) EDS spectrum and element percentage by weight (WT%) and by number of atoms (AT%).

*Mechanical properties*

Typical stress-strain curves of the Col and MC scaffolds obtained by applying 50 cycles of uniaxial compression in wet conditions were shown in Fig 3. Testing was performed at a constant displacement rate until reaching a displacement of 3 mm. The average compressive stress over the 50 cycles was used to calculate the modulus of the scaffold. The Young’s modulus of the MC scaffold was  $0.084 \pm 0.005$  MPa, which was about 2 times higher than that of the Col scaffold ( $0.043 \pm 0.002$  MPa) ( $n = 3$ ) at 50% compression. This result demonstrated that mineralisation resulted in the enhancement of the modulus of the collagen.

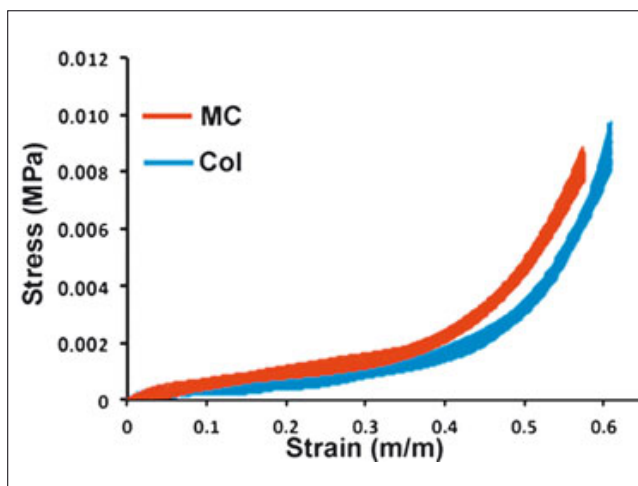


**Fig 3** Typical stress-strain curves of the Col and MC scaffolds obtained by applying 50 cycles of uniaxial compression in wet conditions.

*In vitro cell homing*

The *in vitro* chemotaxis assay showed that the SDF-1 $\alpha$  released from chemokine-loaded scaffolds could attract BMSCs’ migration from the top to the bottom of the transwells (Fig 4). The number of migratory BMSCs induced by the SDF-1-loaded MC scaffold ( $76.2 \pm 8.2$ ) was significantly increased in comparison with the SDF-1 $\alpha$ -loaded Col scaffold ( $30.6 \pm 6.1$ ) and the negative control group ( $13.0 \pm 5.4$ ) ( $P < 0.05$ ). However, compared with the number of the cells migrated in the presence of 200 ng/ml unbound SDF-1 in solution ( $114.2 \pm 11.6$ ), the number of those migrated by the released SDF-1 $\alpha$  from chemokine-loaded scaffolds was much lower ( $P < 0.05$ ).

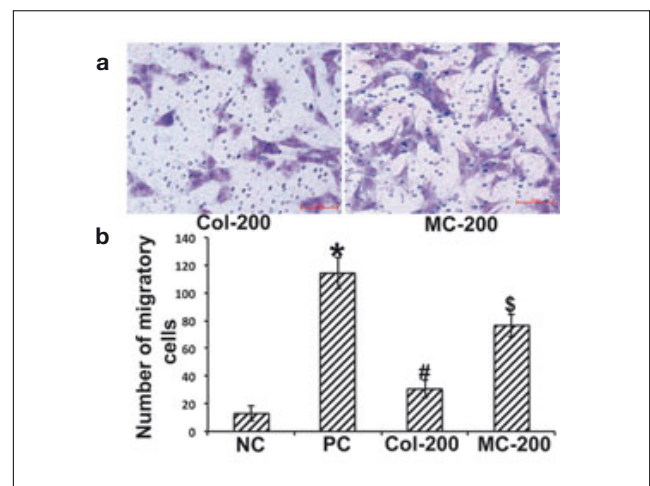


**Fig 4** The chemotaxis effect of SDF-1 $\alpha$  on BMSCs migration. (a) Representative crystal violet-stained images of migratory BMSCs with SDF-1 $\alpha$ -loaded Col scaffold (top left panel) and MC scaffold (top right panel) being placed in the lower chamber. (b) Quantity of migratory cells *in vitro* cell homing assay. \*:  $P < 0.05$  versus NC; #:  $P < 0.05$  versus PC; \$:  $P < 0.05$  versus all of the other groups, by one-way ANOVA. NC: negative control; PC: positive control; Col-200, SDF-1 $\alpha$ -loaded Col scaffold with concentration of 200 ng/ml; MC-200, SDF-1 $\alpha$ -loaded MC scaffold with concentration of 200 ng/ml.

This demonstrated that the loaded SDF-1 $\alpha$  could not be completely released from the chemokine-loaded scaffolds.

### Histological analysis of bone regeneration

To test whether the MC scaffolds function in large bone defect repair *in vivo*, the MC scaffolds (5 mm in diameter) loaded 200 ng/ml SDF-1 $\alpha$  were implanted in 5 mm-diameter rat mandible bone defects (Fig 5). Histopathological analysis of bone regeneration after 12 weeks was performed in HE (Fig 6) and Masson's trichrome staining sections (Fig 7). HE staining showed that more newly formed bone tissue could be observed in the MC group than the Col group. In addition, plenty of residual scaffolds could be seen in the defect region (Fig 6e), and a large amount of ingrowth blood vessels could be found inside the residual scaffolds in the MC group (star). Very limited amount of newly formed bone restricted to areas

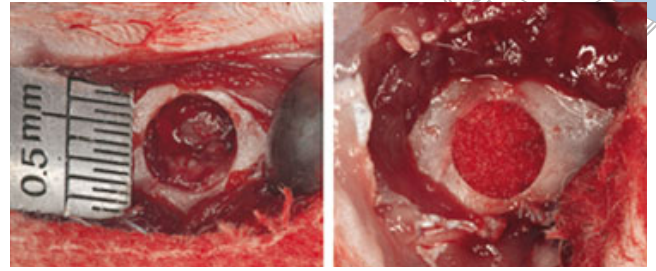


**Fig 5** Surgical procedure of the critical size defect (CSD). (a) Full thickness CSD of 5 mm in diameter. (b) The mandibular defect was filled with collagen scaffold loaded with SDF-1 $\alpha$ .

close to the defect margin and small amount of residual scaffolds was observed in the Col group. When no scaffolds were implanted in the control group, the defect sites were mostly filled with fibrous connective tissue.

Goldner's Masson trichrome staining was also applied to selectively visualise newly formed bone tissue and residual scaffolds (Fig 7)<sup>24</sup>. In this method, the

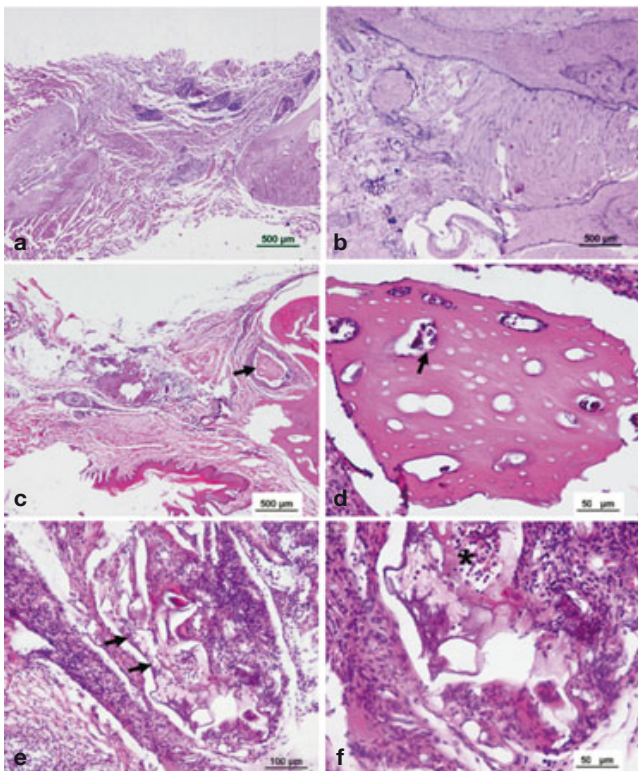


**Fig 6** Histological images of the mandibular bone defect sites by HE staining. (a) Control group, the defect site was filled with fibrous tissue. (b) Col group, few new generated bone tissue with plenty of fibrous tissue. (c) MC group, large amounts of newly formed bone tissue. (d) Magnification of (c), showing bone marrow in newly formed bone tissue (arrow). (e) MC group. Arrows: residual scaffolds. (f) Magnification of (e). Star: blood cells.

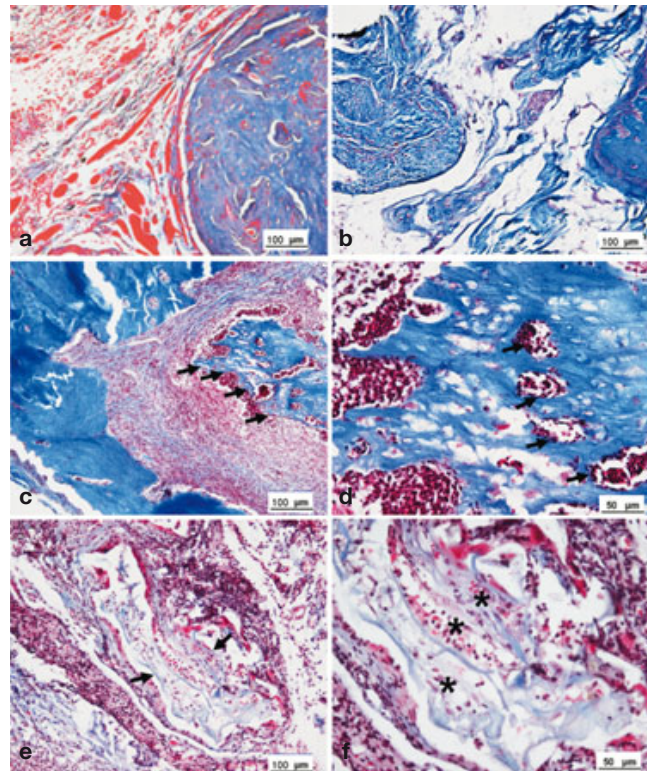


**Fig 7** Masson trichrome staining of the mandibular bone defect sites. (a) Control group, the defect site was filled with myofibre (red). (b) Col group, few new generated bone tissue with plenty of fibrous tissue. (c) MC group, showing newly formed bone tissue (arrows). (d) Magnification of (c), showing bone marrow in newly formed bone tissue (arrows). (e) MC group, showing blood vessels inside the residual scaffolds (arrows). (f) Magnification of (e). Stars: blood cells and vessels.

combination of three different staining solutions with different molecular sizes can stain regenerated tissue differentially. Staining on bone tissue depends on the degree of mineralisation, for instance, mature bone tissue can be stained to brick red, immature bone tissue to light blue or in between. In the MC and Col group, the defect margin was stained to light blue, while in the control group, it was stained to red and blue. This indicated that the osteogenic event was in both scaffold-implanted groups. The color blue, indicating newly formed bone, was distinct in Goldner's Masson trichrome staining. Increased new bone formation was observed in the MC group compared with the Col group. Areas near the defect margin showed a high degree of direct contact with the newly formed bone and plenty of residual scaffolds could be seen with a large amount of ingrowth blood vessels (stars) in the MC group.

## Discussion

Osteoconductive scaffolds and growth factors are of great importance for bone tissue engineering<sup>25</sup>. It has been shown that mineralized collagen fibrils constitute the basic structure of collagenous mineralised tissues such as bone and teeth<sup>26</sup>. Therefore, the MC scaffold, fabricated by biomimetic approach, is thought to be an ideal candidate for bone regeneration. In this study, the biomimetic MC scaffold was prepared by a synchronous precipitation process, in which the collagen molecules self-assembled into fibrils and the amorphous calcium phosphate transformed into crystalline apatites at the same time<sup>16,27</sup>. After collection of the mineralised collagen fibrils by centrifugation, 3D porous scaffolds were produced applying a freeze-drying process<sup>18</sup>, which mimics the extracellular matrix of bone tissue.

Mineralisation has been proven to improve mechanical properties and biological activities of collagen scaffolds such as initial cell adhesion, morphology, proliferation and differentiation in 2D thin collagen film<sup>16</sup>. However, the stiffness of 3D collagen scaffolds was much lower than that of the single collagen fibril. This may be attributed to the high porosity of the scaffold, with those porous extrafibrillar spaces filled with water during testing. In order to maximise bone regeneration *in vivo*, SDF-1 $\alpha$ , which is a major cytokine regulating stem cell homing and inflammatory cell recruitment, was loaded on the scaffolds to create a matrix environment conducive to stem cell migration to the mandibular bone defect area<sup>28</sup>. The *in vitro* cell homing experiments showed that SDF-1 $\alpha$  could be released from chemokine-loaded scaffolds and induced BMSCs' migration.

In our *in vivo* study, increased regenerated bone with activated osteoblast and residual scaffolds was observed in the MC group, while the histological appearance of the Col group and control group showed fibrous tissue and non-active osteoblast along the defect margin. This is in accordance with our previous *in vitro* study that mineralisation could improve the osteogenic potential of collagen scaffolds<sup>16</sup>. In addition, plenty of residual scaffolds could be observed in the MC group. This further confirms that mineralisation can protect collagen from degradation<sup>29</sup>. The delayed degradation of scaffold may be beneficial for further osteogenesis, since the defect area has not been fully repaired. Moreover, we also found a large amount of ingrowing blood vessels inside the MC scaffolds, which indicates that the vascularization degree of the collagen scaffolds can also be improved after mineralisation.

The blood supply to the mandible in rats is limited, which makes it even harder to regenerate than other hard tissue such as skull bone<sup>30</sup>. Findings in this research prove that the MC scaffold is a promising candidate for TE scaffolds. This scaffold can not only promote osteogenesis, but also provide adequate repair time and an affluent blood supply. Therefore, within the limits of the present study, it may be concluded that the MC scaffold, loaded with SDF-1 $\alpha$  creating a matrix environment conducive to stem cell migration, can be exploited to improve bone regeneration as an alternative to contemporary cell seeding approaches. Further research should be directed toward the fabrication of 3D porous collagen scaffolds with a hierarchical nanostructure to natural bone to achieve more satisfactory bone regeneration.

## References

1. Zamiri B, Shahidi S, Eslaminejad MB, et al. Reconstruction of human mandibular continuity defects with allogenic scaffold and autologous marrow mesenchymal stem cells. *J Craniofac Surg* 2013;24:1292–1297.
2. Chim H, Salgado CJ, Mardini S, Chen HC. Reconstruction of mandibular defects. *Semin Plast Surg* 2010;24:188–197.
3. Canter HI, Vargel I, Mavili ME. Reconstruction of mandibular defects using autografts combined with demineralized bone matrix and cancellous allograft. *J Craniofac Surg* 2007;18:95–100; discussion 101–103.
4. Terheyden H, Warnke P, Dunsche A, et al. Mandibular reconstruction with prefabricated vascularized bone grafts using recombinant human osteogenic protein-1: an experimental study in miniature pigs. Part II: transplantation. *Int J Oral Maxillofac Surg* 2001;30:469–478.
5. Akbay E, Aydogan F. Reconstruction of isolated mandibular bone defects with non-vascularized corticocancellous bone autograft and graft viability. *Auris Nasus Larynx* 2014;41:56–62.
6. Zhang L, Zhou J, Lu Q, et al. A novel small-diameter vascular graft: *in vivo* behavior of biodegradable three-layered tubular scaffolds. *Biotechnol Bioeng* 2008;99:1007–1015.

7. Lu HH, El-Amin SF, Scott KD, Laurencin CT. Three-dimensional, bioactive, biodegradable, polymer-bioactive glass composite scaffolds with improved mechanical properties support collagen synthesis and mineralization of human osteoblast-like cells in vitro. *J Biomed Mater Res A* 2003;64:465–474.
8. Qian J, Suo A, Jin X, et al. Preparation and in vitro characterization of biomorphic silk fibroin scaffolds for bone tissue engineering [epub ahead of print 30 Sep 2013]. *J Biomed Mater Res A*. doi: 10.1002/jbm.a.34964.
9. Schantz JT, Chim H, Whiteman M. Cell guidance in tissue engineering: SDF-1 mediates site-directed homing of mesenchymal stem cells within three-dimensional polycaprolactone scaffolds. *Tissue Eng* 2007;13:2615–2624.
10. Ren T, Ren J, Jia X, Pan K. The bone formation in vitro and mandibular defect repair using PLGA porous scaffolds. *J Biomed Mater Res A* 2005;74:562–569.
11. Hollister SJ. Porous scaffold design for tissue engineering. *Nat Mater* 2005;4:518–524.
12. Wang Q, Jamal S, Detamore MS, Berklund C. PLGA-chitosan/PLGA-alginate nanoparticle blends as biodegradable colloidal gels for seeding human umbilical cord mesenchymal stem cells. *J Biomed Mater Res A* 2011;96:520–527.
13. Chevally B, Herbage D. Collagen-based biomaterials as 3D scaffold for cell cultures: applications for tissue engineering and gene therapy. *Med Biol Eng Comput* 2000;38:211–218.
14. Tsai SW, Liou HM, Lin CJ, et al. MG63 osteoblast-like cells exhibit different behavior when grown on electrospun collagen matrix versus electrospun gelatin matrix. *PLoS One* 2012;7:e31200.
15. Aravamudan A, Ramos DM, Nip J, et al. Cellulose and collagen derived micro-nano structured scaffolds for bone tissue engineering. *J Biomed Nanotechnol* 2013;9:719–731.
16. Liu Y, Luo D, Kou XX, et al. hierarchical intrafibrillar nanocarbonated apatite assembly improves the nanomechanics and cytocompatibility of mineralized collagen. *Advan Funct Mater* 2013;23:1404–1411.
17. Bernhardt A, Lode A, Boxberger S, et al. Mineralised collagen – an artificial, extracellular bone matrix – improves osteogenic differentiation of bone marrow stromal cells. *J Mater Sci Mater Med* 2008;19:269–275.
18. Yokoyama A, Gelinsky M, Kawasaki T, et al. Biomimetic porous scaffolds with high elasticity made from mineralized collagen – an animal study. *J Biomed Mater Res B Appl Biomater* 2005;75:464–472.
19. Bernhardt A, Lode A, Mietrach C, et al. In vitro osteogenic potential of human bone marrow stromal cells cultivated in porous scaffolds from mineralized collagen. *J Biomed Mater Res A* 2009;90:852–862.
20. Niu LN, Jiao K, Qi YP, et al. Intrafibrillar silicification of collagen scaffolds for sustained release of stem cell homing chemokine in hard tissue regeneration. *FASEB J* 2012;26:4517–4529.
21. He X, Ma J, Jabbari E. Migration of marrow stromal cells in response to sustained release of stromal-derived factor-1alpha from poly(lactide ethylene oxide fumarate) hydrogels. *Int J Pharm* 2010;390:107–116.
22. Sadir R, Baleux F, Grosdidier A, et al. Characterization of the stromal cell-derived factor-1alpha-heparin complex. *J Biol Chem* 2001;276:8288–8296.
23. Maniopoulos C, Sodek J, Melcher AH. Bone formation in vitro by stromal cells obtained from bone marrow of young adult rats. *Cell Tissue Res* 1988;254:317–330.
24. Gruber HE. Adaptations of Goldner's Masson trichrome stain for the study of undecalcified plastic embedded bone. *Biotech Histochem* 1992;67:30–34.
25. Paderni S, Terzi S, Amendola L. Major bone defect treatment with an osteoconductive bone substitute. *Chir Organi Mov* 2009;93:89–96.
26. Weiner S, Addadi L. Design strategies in mineralized biological materials. *J Mater Chem* 1997;7:689–702.
27. Gelinsky M, Welzel PB, Simon P, et al. Porous three-dimensional scaffolds made of mineralised collagen: preparation and properties of a biomimetic nanocomposite material for tissue engineering of bone. *Chem Eng J* 2008;137:84–96.
28. Zhou SB, Wang J, Chiang CA, et al. Mechanical stretch upregulates Sdf-1alpha in skin tissue and induces migration of circulating bone marrow-derived stem cells into the expanded skin. *Stem Cells* 2013;31:2703–2713.
29. Trebacz H, Wojtowicz K. Thermal stabilization of collagen molecules in bone tissue. *Int J Biol Macromol* 2005;37:257–262.
30. Kantomaa T. Growth of the mandible. An experimental study in the rat. *Proc Finn Dent Soc* 1984;80:58–66.